

BLAEs – I. Resolving the UV-continuum in Lyman alpha emitting galaxies between redshift 2 to 3 with gravitational lensing

E. Ritondale,¹ A. N. Other,² Third Author^{2,3} and Fourth Author³

¹Max Planck Institute for Astrophysics, Karl-Schwarzschild-Strasse 1, D-85740 Garching, Germany

Accepted XXX. Received YYY; in original form ZZZ

ABSTRACT

Lyman-alpha emitters (LAEs) are low-mass, high specific star formation rate galaxies that are thought to be predominantly responsible for the reionisation of the Universe. In spite of their importance, it is extremely difficult to characterise in detail all but the brightest, most massive of these galaxies; this is unsatisfactory, since the faint LAE population is expected to contribute significantly to the reionisation. Here we present a study of a new sample of 20 strongly lensed Ly- α emitting galaxies at $z \sim 2.3$, where we take advantage of the lensing magnification (typically a factor of about 20) to characterise some of the physical properties of low star-formation rate LAEs for the first time.

Key words: gravitational lensing – galaxies: structure

1 INTRODUCTION

Lyman-alpha emitting galaxies (LAEs) represent a population of star-forming systems with very large Ly α equivalent widths and some of the highest specific star-formation rates (sSFR) in the Universe, and these low-mass galaxies are thought to be predominantly responsible for the reionisation of the Universe. However, it is extremely difficult to characterise these galaxies in detail because they are intrinsically very faint. Typical LAE galaxies have strong star-formation, high-ionisations, and are typically low metallicity; these properties, combined with a (mostly) low dust content, allow for the escape of a large fraction of Ly α photons. At redshift $2 < z < 3$, well-studied LAEs are typically at the bright end of this parameter space, being L* galaxies with $M_* \sim 10^9 M_\odot$ and typical SFRs of about 30 to $100 M_\odot/\text{yr}$ (e.g. Erb et al. 2016), and investigations of lower-SFR objects have generally been limited to quantifying the properties of strong optical lines (e.g. Trainor et al. 2015). For example, Hagen et al. (2016) have recently shown that low-SFR LAEs (M_* as low as $10^7 M_\odot$ and SFR ~ 1 to $100 M_\odot/\text{yr}$, consistent with local-Universe *green pea* LAEs, e.g., Henry et al. 2015) have optical strong line (H_α and [O iii]) properties consistent with optically-selected star-forming galaxies of the same masses at $z \sim 2$, but they are unable to directly determine the properties of these galaxies that may affect the UV escape fraction, including the gas metallicity, density, and kinematics, without additional very large investments in telescope time.

Strong gravitational lensing can be used to overcome this limitation, but the difficulty is that most strongly lensed galaxies at $z \sim 2$ are not LAEs, and at present the properties of only three lensed

LAEs have been investigated in detail (Christensen et al. 2012; Vanzella et al. 2016). Fortunately, new HST V-band observations of LAE galaxies selected from the BOSS survey have revealed a sample of strongly lensed systems at $\langle z \rangle \sim 2.5$ for which the magnification effect could reveal the detailed structure of these LAEs at scales around 100 pc. Our subsequent lens modelling shows that the typical lensing magnification of these objects is $\mu \sim 20$ and, after accounting for this magnification, these objects are compact galaxies with SFRs of $\sim 12 M_\odot/\text{yr}$ (i.e., a factor of 3 to 8 lower than previous detailed studies).

In this paper, we use strong gravitational lensing to go beyond the current limits in angular resolution to investigate the size and structure of Lyman alpha emitting galaxies at high redshift on 100–500 pc-scales. Our study is based on the sample of candidate gravitational lenses that were selected from the BOSS Emission Line Lens Survey (BELLS) by Shu et al. (2016a). To summarise, 1.4×10^6 galaxy spectra from the Baryon Oscillation Spectroscopic Survey (BOSS) of the Sloan Digital Sky Survey-III were inspected to search for Lyman alpha emission lines at a higher redshift than the dominant early-type galaxy in the spectrum. From this search, Shu et al. (2016a) selected twenty-one highest quality targets with source redshifts between $z \sim 2$ to 3 for follow-up imaging with the *HST*. This selection method is based on the successful technique used by the Sloan Lens ACS Survey (SLACS) to find over eighty-five gravitational lensed star-forming galaxies at lower redshifts (Auger et al. 2009; Bolton et al. 2008), and has recently been applied by Shu et al. (2016b) to find a Lyman alpha emitting galaxy at redshift 2.701 that is gravitationally lensed by two elliptical galaxies at redshift 0.331.

Our paper is arranged as follows. In Section 2, we present the high angular resolution *HST* observations of the rest-frame ultraviolet continuum emission from the BELLS sample of candidate

* E-mail: elisa@mpa-grarching.mpg.de

Lyman alpha emitting galaxies, from which we select the seventeen sources of our BOSS Lyman alpha emitters (BLAEs) sample. Using these data, the gravitational lens mass models and reconstructed source surface brightness distributions of the sample are determined in Section 3. From these source reconstructions, we investigate the intrinsic properties of the rest-frame ultra-violet continuum emission from the sample in Section 4. Here, we also study the properties of the stacked optical spectrum of the sample. We compare with other samples of Lyman alpha emitters in the literature and discuss our results in Section 5. Finally, in Section 6 we present our conclusions.

2 OBSERVATIONS

The BELLS sample was observed with the *HST* using the WFC3 camera and the F606W filter ($\lambda_c = 5887 \text{ \AA}$; $\Delta\lambda = 2182 \text{ \AA}$) between 2015 November and 2016 May (GO: 14189; PI: Bolton). In total, twenty one candidate gravitationally lensed Lyman-alpha emitting galaxies from the Shu et al. (2016a) sample were observed for about 2600 s each. As their redshifts span from $z \sim 2.1$ to 2.8 and given the transmission curve of the F606W filter, these observations probed the rest-frame ultraviolet emission from young massive stars between 1250 and 2230 \AA .

The data were retrieved from the *HST* archive and processed using the ASTRODRIZZLE task that is part of the DRIZZLEPAC package. Cut-out images for each target are shown in Fig. 1. Out of the twenty one candidates, three turned out not to be strong gravitational lenses with clear multiple images of the same background galaxy (SDSS J0054+2944, SDSS J1116+0915 and SDSS J1516+4954). Also, SDSS J2245+0040 is not included in our final sample because the uncertain nature of the deflector, which appears to be a spiral galaxy, made identifying the emission from the lensed Lyman alpha emitting galaxy challenging without additional colour information. Therefore, the final BLAEs sample used for our analysis contains seventeen gravitationally lensed Lyman-alpha emitting galaxies. The details of the sources in our final sample and the *HST* data that we will use are given in Table 1.

3 GRAVITATIONAL LENS MODELLING

3.1 Lens modelling procedure

The gravitational lens modelling and source reconstruction of each system was performed using a new version of the Bayesian pixelated technique developed by Vegetti & Koopmans (2009).

Consider the observed surface brightness distribution \mathbf{d} given by the combination of the lensed image \mathbf{d}_s of an unknown extended background source s and the surface brightness distribution of the lensing galaxy \mathbf{d}_l . Both \mathbf{d}_s and s are vectors representing the surface brightness distribution on a set of pixels, on the lens plane and source plane, respectively. The grid on the lens plane is defined by the native CCD pixelation of the data, while the grid on the source plane is defined by a magnification-adaptive Delaunay tessellation (see Vegetti & Koopmans 2009, for more details). This provides a pixellated surface brightness distribution for the reconstructed source that is free from any parameterized assumptions, such as Sersic or Gaussian light profiles, that may not fully account for the clumpy nature of the rest-frame ultraviolet emission from the BLAEs sources.

The positions of the pixels are related between the two planes by the lensing equation via the projected gravitational potential

$\psi(x, \boldsymbol{\eta})$ of the lensing galaxy, defined by the unknown parameters $\boldsymbol{\eta}$. Taking advantage of the fact that gravitational lensing conserves surface brightness and taking into account for the observational noise \mathbf{n} , then \mathbf{d} and s can be related to each other via a set of linear equations,

$$[\mathbf{BL}(x, \boldsymbol{\eta}) + \lambda \mathbf{R} | \mathbf{BI}(x, \boldsymbol{\eta}_l) | \mathbf{1}] \begin{pmatrix} s \\ I_0 \\ C \end{pmatrix} = \begin{pmatrix} \mathbf{d}_s \\ \mathbf{d}_l \\ \mathbf{n} \end{pmatrix}. \quad (1)$$

Here, \mathbf{B} is the blurring operator that expresses the effect of the point spread function. \mathbf{R} and λ are respectively the form and unknown level of the source surface brightness distribution regularization and are essentially a form of prior on the level of smoothness of the background galaxy. C is a constant pedestal, expressing the sky background. $\mathbf{I}(x, \boldsymbol{\eta}_l)$ is the surface brightness distribution of the foreground gravitational lens, which is simultaneously modelled with the mass distribution and is parametrized using elliptical Sersic profiles of total normalization I_0 , effective radius R_e , Sersic index n and axis ratio b , such that,

$$I(x) = I_0 \exp \left[\left(-b n \left(\frac{r}{R_e} \right)^{1/n} \right) - 1.0 \right]. \quad (2)$$

We refer to the Sersic parameters collectively as $\boldsymbol{\eta}_l$. \mathbf{L} is the lensing operator and is related via the lens equation to the lens mass distribution. The latter is parametrized with an elliptical power-law profile of dimensionless surface mass density κ , given by,

$$\kappa(x, y) = \frac{\kappa_0 \left(2 - \frac{\gamma}{2} \right) q^{\gamma-3/2}}{2 \left(q^2 (x^2 + r_c^2) + y^2 \right)^{(\gamma-1)/2}}, \quad (3)$$

where κ_0 is the surface mass density normalization, q is the axial ratio of the elliptical mass distribution, γ is the radial slope of the mass density profile and r_c is the core-radius. In addition, the position angle of the elliptical mass distribution (θ), and the shear strength (Γ) and positional angle (Γ_θ) are also solved for. We refer to the mass density parameters collectively as $\boldsymbol{\eta}$. The dimensionless surface mass density and the Einstein radius (R_{ein}) are related to each other via,

$$R_{\text{ein}} = \left(\frac{\kappa_0 \left(2 - \frac{\gamma}{2} \right) q^{(\gamma-2)/2}}{3 - \gamma} \right)^{1/(\gamma-1)}. \quad (4)$$

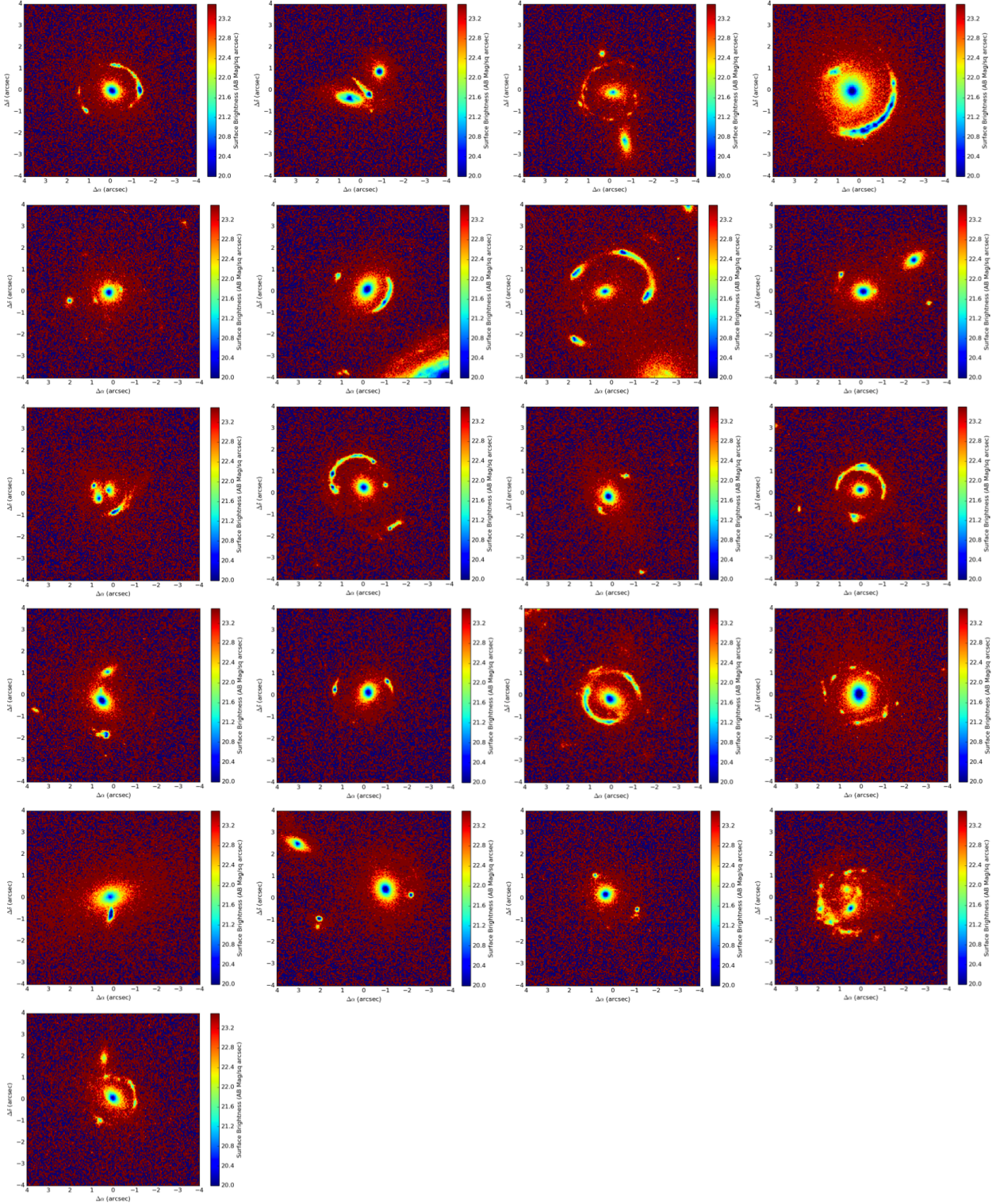
The modelling procedure is performed in three steps: first we masked out the emission from the lens galaxy and, given the lensed surface brightness distribution \mathbf{d} , we optimize for the lens mass parameters $\boldsymbol{\eta} = \{\kappa_0, \theta, q, x, y, \gamma, \Gamma, \Gamma_\theta\}$ and the source regularization level by maximizing the posterior probability density,

$$P(\lambda_s, \boldsymbol{\eta} | \mathbf{d}, \mathbf{R}_s) = \frac{P(\mathbf{d} | \lambda_s, \boldsymbol{\eta}, \mathbf{R}_s) P(\lambda_s, \boldsymbol{\eta})}{P(\mathbf{d} | \mathbf{R}_s)}. \quad (5)$$

At each step of this optimization, the corresponding most probable source s is obtained by maximizing the probability density distribution,

$$P(s | \mathbf{d}, \lambda_s, \boldsymbol{\eta}, \mathbf{R}_s) = \frac{P(\mathbf{d} | s, \boldsymbol{\eta}) P(s | \lambda_s, \mathbf{R}_s)}{P(\mathbf{d} | \lambda_s, \boldsymbol{\eta}, \mathbf{R}_s)}. \quad (6)$$

Then, using this as a starting point, we parametrize the surface brightness distribution of the lens galaxy as a sum of multiple elliptical Sersic profiles, and optimize for the corresponding parameters, $\boldsymbol{\eta}_l = \{I_0, R_e, n, b, \theta\}$, together with the background source surface brightness distribution. In the third and final step, we optimize simultaneously for the mass and the light distribution of the deflector and the source regularization level.



The resulting models for the lens- and source-plane light distributions are presented in Fig. 2, the Einstein radius, enclosed lensing mass and the source magnification for each system are given in Table 1 and the Sersic surface brightness distributions of the lensing galaxies are given in Table 2. The source magnifications have been calculated by dividing the total flux in the lens plane by the total flux in the source plane.

3.2 Notes on the individual lens models

4 INTRINSIC PROPERTIES OF THE RECONSTRUCTED LAE GALAXIES

5 DISCUSSION

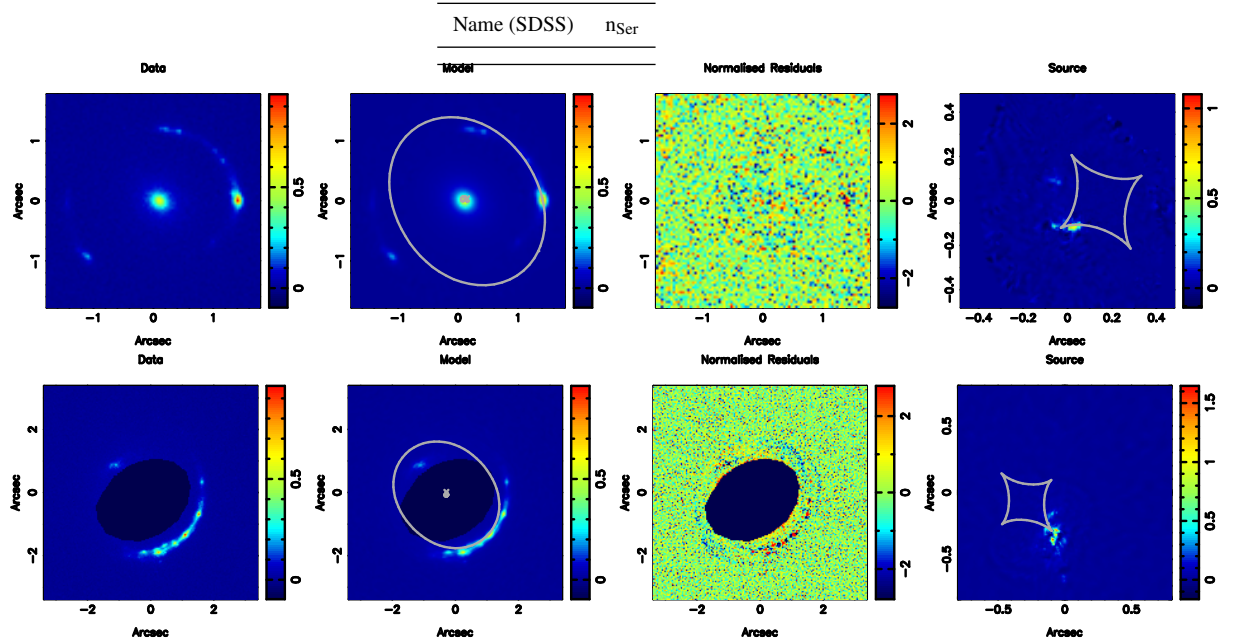
6 CONCLUSIONS

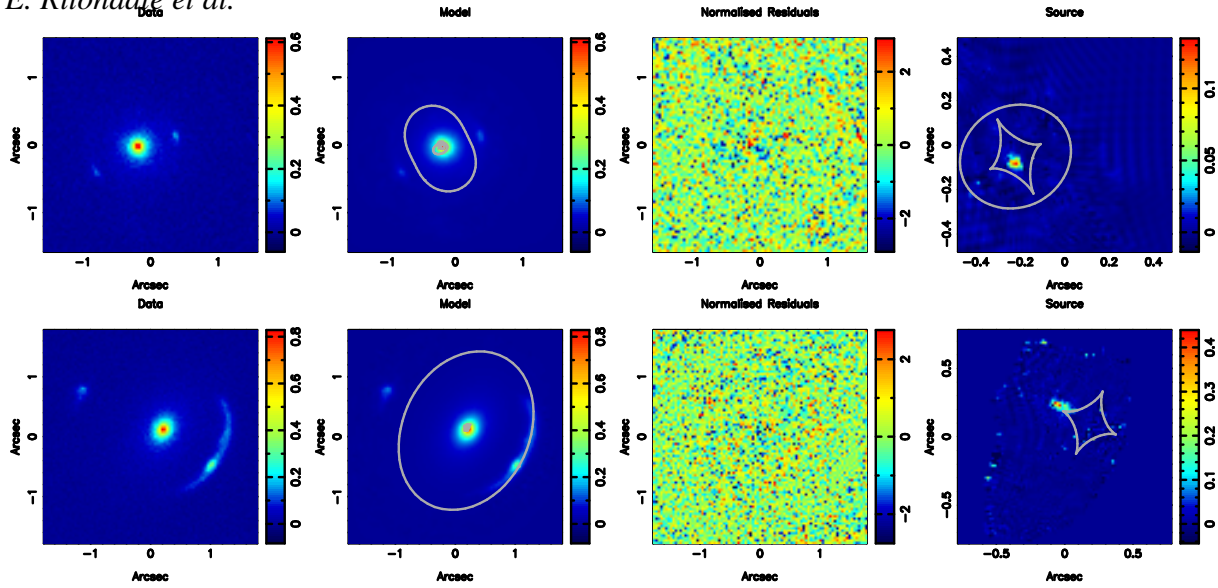
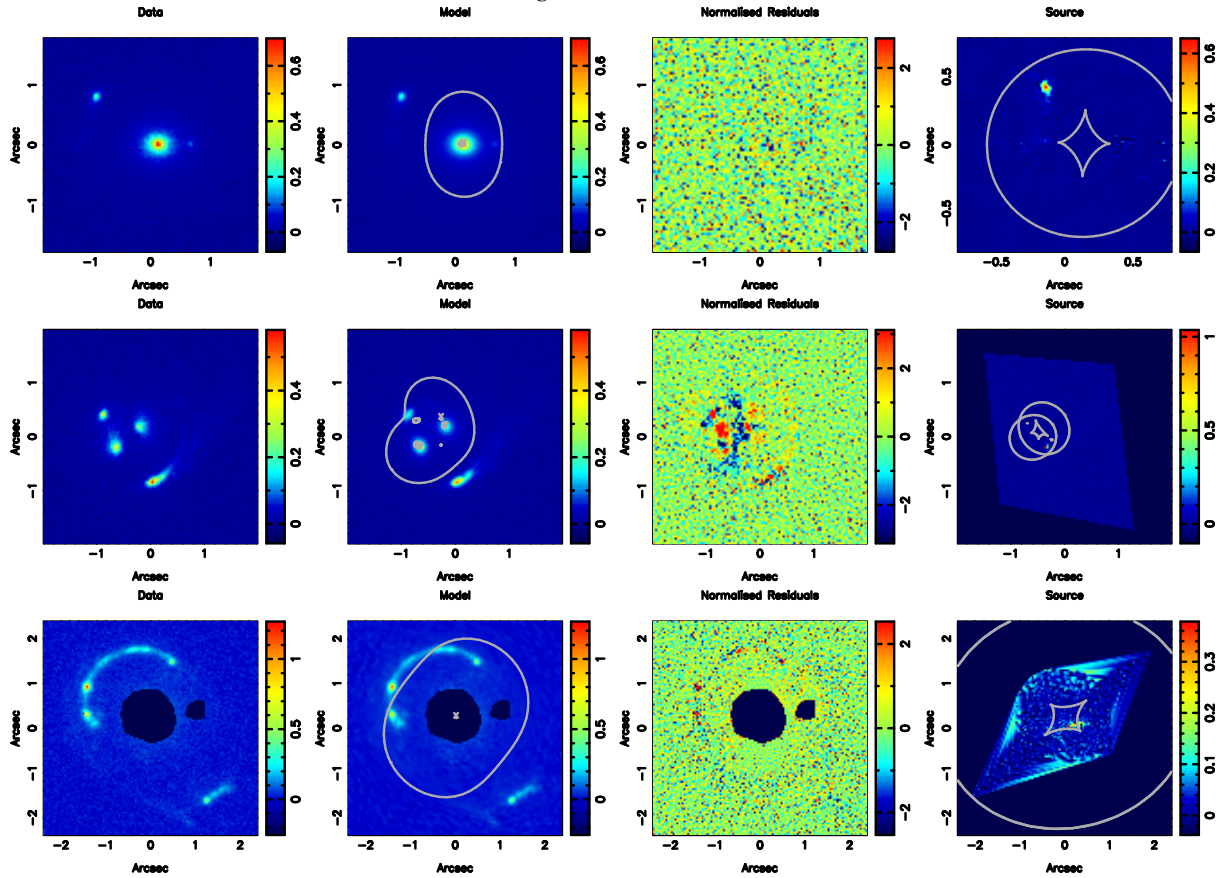
REFERENCES

- Auger M. W., Treu T., Bolton A. S., Gavazzi R., Koopmans L. V. E., Marshall P. J., Bundy K., Moustakas L. A., 2009, [ApJ, 705, 1099](#)
 Bolton A. S., Burles S., Koopmans L. V. E., Treu T., Gavazzi R., Moustakas L. A., Wayth R., Schlegel D. J., 2008, [ApJ, 682, 964](#)
 Shu Y., et al., 2016a, preprint, ([arXiv:1604.01842](#))
 Shu Y., Bolton A. S., Moustakas L. A., Stern D., Dey A., Brownstein J. R., Burles S., Spinrad H., 2016b, [ApJ, 820, 43](#)
 Vegetti S., Koopmans L. V. E., 2009, [MNRAS, 392, 945](#)
 Vegetti S., Koopmans L. V. E., Auger M. W., Treu T., Bolton A. S., 2014, [MNRAS, 442, 2017](#)

Table 1. Details of the BLAEs sample used for our analysis and the derived gravitational lens mass models.

Name (SDSS)	z_{lens}	z_{src}	$\lambda_{\text{rest}} [\text{\AA}]$	Exp. Time [s]	R_{ein} [arcsec]
J0029 + 2544	0.587	2.450	1706	2504	1.330
J0113 + 0250	0.623	2.609	1631	2484	1.225
					0.070
					0.173
J0201 + 3228	0.396	2.821	1540	2520	
J0237 – 0641	0.486	2.249	1812	2488	0.536
J0742 + 3341	0.494	2.363	1751	2520	1.208
J0755 + 3445	0.722	2.634	1620	2520	
J0856 + 2010	0.507	2.233	1821	2496	0.745
J0918 + 4518	0.524	2.344	1761	2624	
J0918 + 5104	0.581	2.403	1730	2676	
J1110 + 2808	0.607	2.399	1732	2504	0.985
J1110 + 3649	0.733	2.502	1682	2540	1.145
J1141 + 2216	0.586	2.762	1565	2496	1.281
J1201 + 4743	0.563	2.126	1883	2624	1.186
J1226 + 5457	0.498	2.732	1578	2676	
J1529 + 4015	0.531	2.792	1553	2580	
J2228 + 1205	0.530	2.832	1536	2492	1.270
J2342 – 0120	0.527	2.265	1803	2484	1.088

Table 2. Add caption here. This table should contain the best parameters for the sersic models**Figure 2.** Models for the BLAEs gravitational lens systems. Each row shows (left) the input *HST* F606W imaging, (middle-left) the reconstructed model for lens-plane surface brightness distribution of the gravitational lensing galaxy and the gravitationally lensed BLAEs galaxy, (middle-right) the normalised image residuals between $\pm 2.5\sigma$, and (right) the reconstructed surface brightness distribution of the BLAEs galaxy. Shown in grey are the gravitational lens mass model critical curves in the lens-plane and the caustics in the source-plane.

**Figure 2 – continued****Figure 2 – continued**

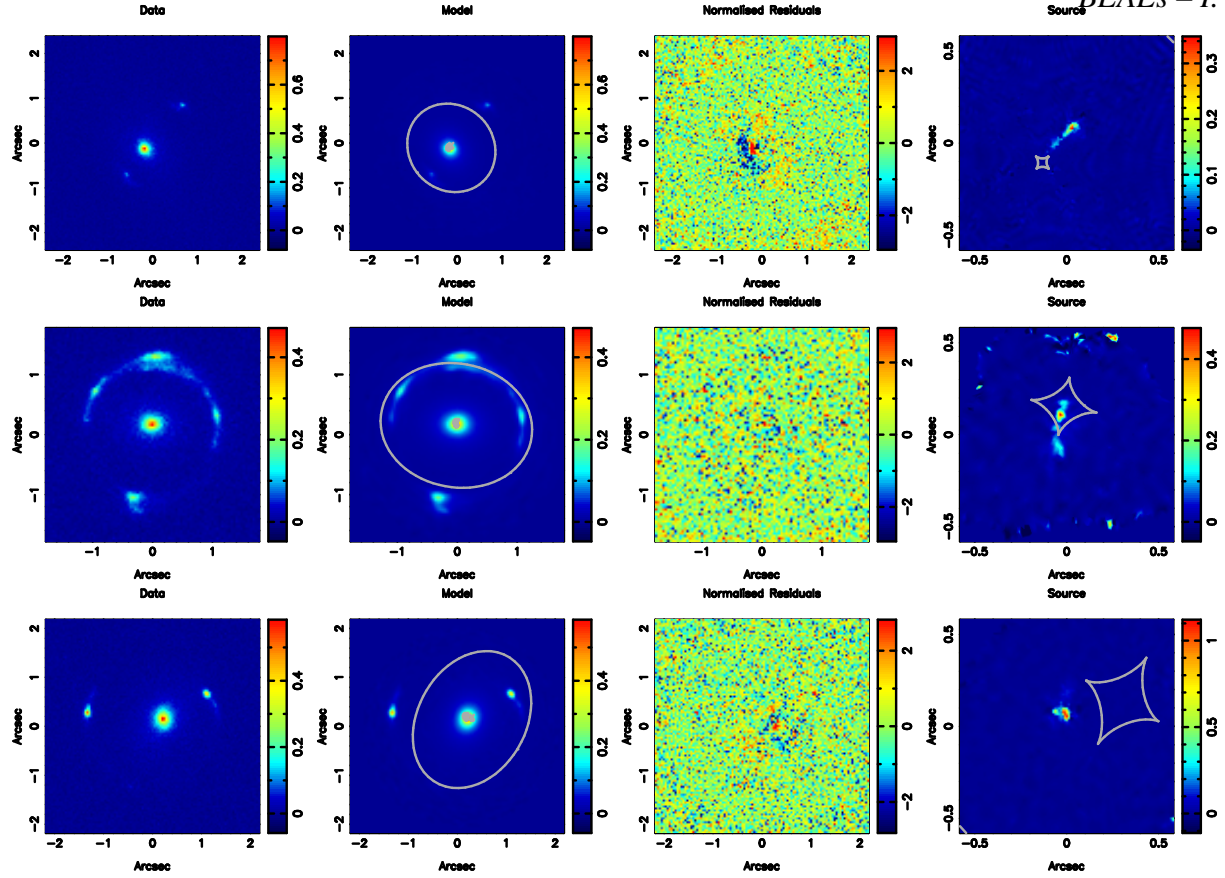
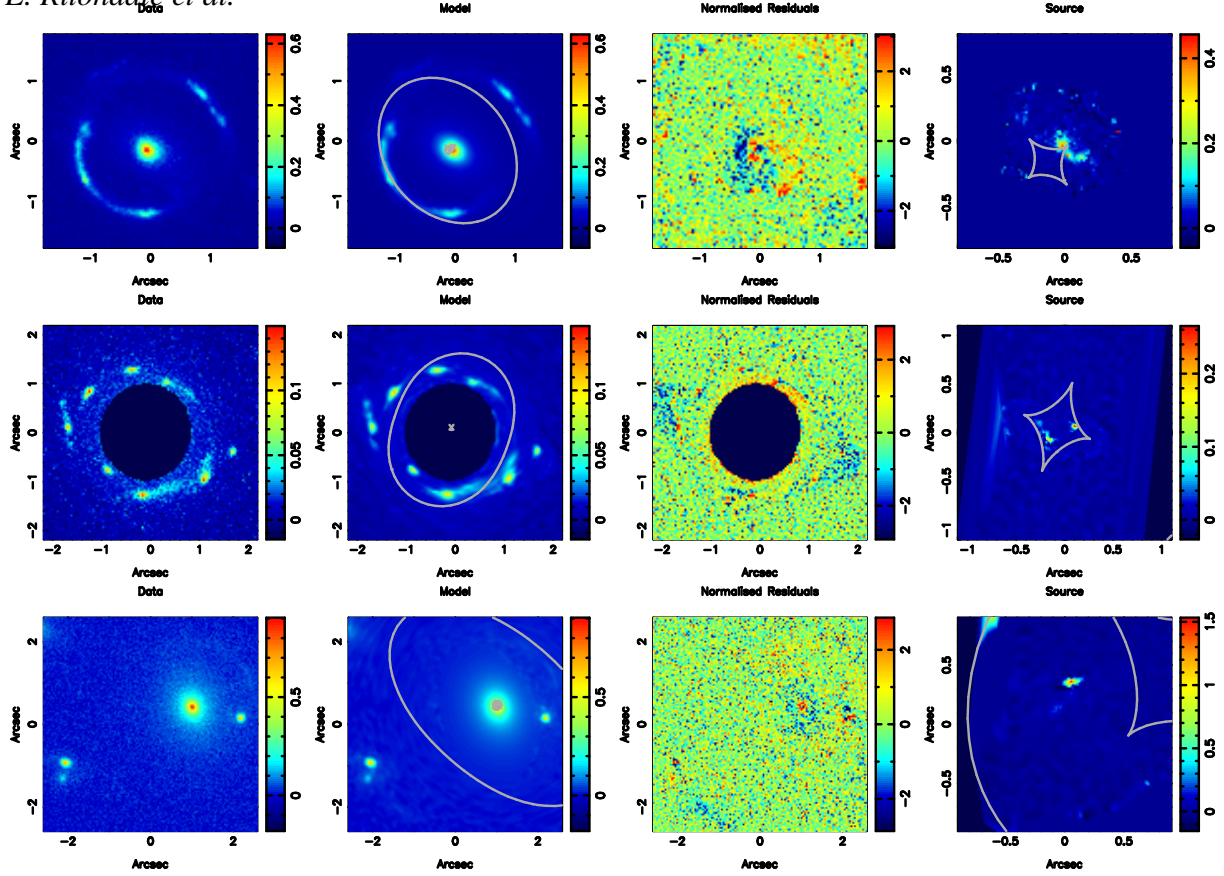
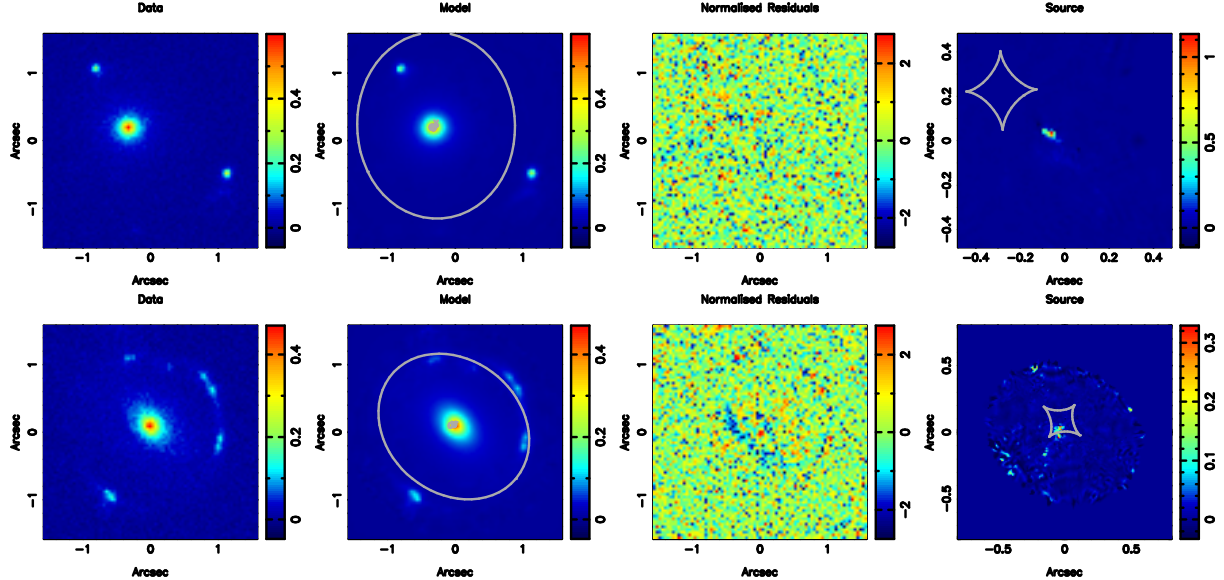


Figure 2 – continued

**Figure 2 – continued****Figure 2 – continued**